Bipolar charging and discharging of a perfectly conducting sphere in a lossy medium stressed by a uniform electric field

J. George Hwang,[1,a)] Markus Zahn,[1] and Leif A. A. Pettersson[2]
[1]*Department of Electrical Engineering and Computer Science, Massachusetts Institute of Technology, 77 Massachusetts Avenue, Room 10-174, Cambridge, Massachusetts 02139 USA*
[2]*ABB Corporate Research S-72178 Västerås, Sweden*

(Received 23 November 2010; accepted 11 February 2011; published online 22 April 2011)

Generalized analysis is presented extending recent work of the charging of a perfectly conducting sphere from a single charge carrier to two charge carriers of opposite polarity, with different values of volume charge density and mobility and including an ohmic lossy dielectric region surrounding a perfectly conducting sphere. Specific special cases treated are: (1) unipolar positive or negative charging and discharging and (2) bipolar charging and discharging; both cases treating zero and nonzero conductivity of the dielectric region surrounding a sphere. It is found that there exists a theoretical limit to the amount of charge, either positive or negative, that can accumulate on a perfectly conducting sphere for a specific applied electric field magnitude, permittivity of the surrounding medium, and sphere size. However, in practice this saturation charge limit is not reached and the sphere is charged to a lower value due to the nonzero conductivity of the surrounding medium and the existence of both positive and negative mobile carriers. Moreover, it is the respective effective conductivities of these positive and negative carriers, as well as the conductivity of the surrounding medium, which strongly influences the sphere's lowered saturation charge limit, charge polarity, charging rate, and discharging rate. © *2011 American Institute of Physics*. [doi:10.1063/1.3563074]

I. INTRODUCTION

Extensive research on transformer oil insulated high-voltage and power apparatus is aimed at improving the electrical breakdown and thermal characteristics.[1] One approach studied transformer oil-based nanofluids with conductive nanoparticle suspensions that defy conventional wisdom, as past measurements have shown that such nanofluids have substantially higher positive voltage breakdown levels with slower positive streamer velocities than those of pure transformer oil.[2–8] This paradoxical superior electric field breakdown performance, compared to that of pure oil, is due to the electron charging of the nanoparticles that convert high-mobility electrons generated by field ionization to slow, negatively charged nanoparticles carrying trapped electrons with effective mobility reduction by a factor of about 1×10^5.[9–13] Recent work has analyzed the unipolar negative charging by electrons of infinite and finite conductivity nanoparticles to show that electron trapping is the cause of the decrease in positive streamer velocity resulting in higher positive electrical breakdown strength. The analysis derived the electric field in the vicinity of the nanoparticles; electron trajectories on electric field lines that terminate on the nanoparticle to negatively charge them; and the charging characteristics of the nanoparticles as a function of time, dielectric permittivity, and conductivity of the nanoparticles and the surrounding oil. This charged nanoparticle model was used with a comprehensive electrodynamic analysis for the charge generation, recombination, and transport of positive and negative ions, electrons, and charged nanoparticles between a positive, high-voltage, sharp needle electrode and a large, spherical ground electrode. Numerical case studies showed that in transformer oil without nanoparticles, field ionization leads to electric field and space charge waves that travel between electrodes, generating enough heat to vaporize the transformer oil to cause a positive streamer that precedes electrical breakdown. When conductive nanoparticles are added to the oil they effectively trap fast electrons, which results in a significant reduction in streamer speed, offering improved high-voltage performance and reliability.

The purpose of this paper is to extend the results of previous work[9–13] from electron unipolar charging of conducting nanoparticle spheres with negligible ohmic conductivity of the surrounding liquid dielectric to bipolar charging and discharging of conducting spheres including ohmic loss of the surrounding dielectric liquid. The analysis considers the bipolar charging and discharging transients of a perfectly conducting sphere after an initial step voltage change from zero in an applied uniform electric field. The analysis extends the analogous Whipple and Chalmers model,[14] originally applied to thunderstorm electrification, but in our case there is no flow of dielectric liquid. Similar modeling has also been used to model ion impact charging used in electrostatic precipitators.[15] Analysis is presented for perfectly conducting spheres with possible applications to electrical breakdown research of conducting nanoparticle spheres in dielectric liquid suspensions.

II. BIPOLAR CHARGING OF A PERFECTLY CONDUCTING SPHERE STRESSED BY AN APPLIED UNIFORM ELECTRIC FIELD

We consider the charging of an isolated, perfectly conducting sphere in an applied uniform electric field. At $t = 0$, the uniform z-directed dc electric field $\vec{E} = E_0\vec{i}_z$ at infinity is turned on within a lossy dielectric with permittivity ϵ and conductivity σ, where we take E_0 to be positive. The

a)Author to whom correspondence should be addressed. Electronic address: ghwang@mit.edu.

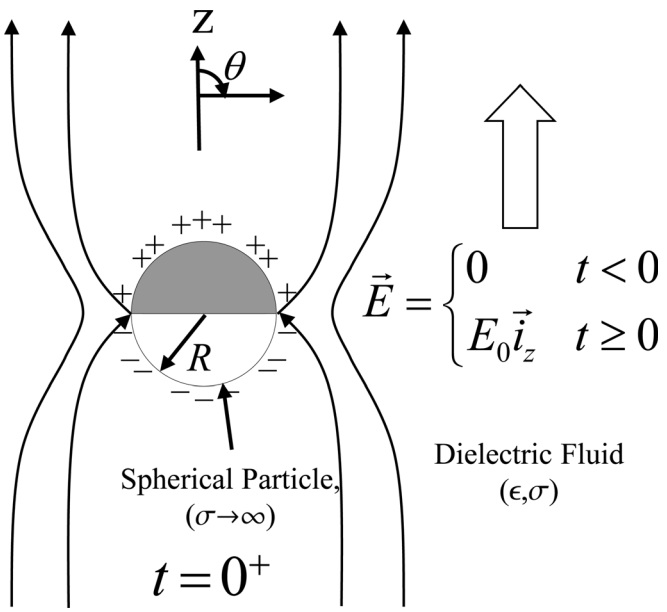

FIG. 1. Electric field lines around a perfectly conducting sphere with radius R surrounded by a dielectric fluid with a permittivity of ϵ and conductivity σ stressed by a uniform z-directed electric field, $\vec{E} = E_0\vec{i}_z$, turned on at $t=0$.

perfectly conducting sphere of radius R centered at $r=0$ distorts the applied uniform electric field by instantaneously adding a dipole electric field due to positive surface charging on the upper $0<\theta<\pi/2$ hemisphere and negative surface charging on the lower $\pi/2<\theta<\pi$ hemisphere, as shown in Fig. 1. We assume that the electric field also ionizes the dielectric region surrounding the sphere with positive charge carriers with charge density ρ_+ and mobility μ_+ and negative charge carriers with charge density ρ_-, which is a negative quantity, and mobility μ_-, where we take μ_+ and μ_- to be positive. These two mobile charge carriers will be driven by the electric field to charge the sphere surface with time-dependent total charge $Q(t)$ to be determined by this analysis.

We assume that the volume charge density from ρ_+ and ρ_- outside the perfectly conducting sphere for $r>R$ is small so that the electric field due to the volume charge density is much less than the applied electric field strength E_0. The electric field for $t>0$ and $r>R$ is determined from solutions to Laplace's equation in spherical coordinates for the electrostatic scalar potential $\Phi(r,\theta,t)$. The total electric field, $\vec{E}(r,\theta,t) = -\nabla\Phi(r,\theta,t)$, is then due to the superposition of the imposed uniform electric field, the induced dipole field from the sphere surface charge with effective dipole moment $\vec{p} = 4\pi\epsilon R^3 E_0\vec{i}_z$, and the Coulomb field from the net charge $Q(t)$ flowing onto the sphere from the mobile positive and negative charges. The electric field for $t>0$ is then

$$\vec{E}(r,\theta,t) = \left[E_0\left(1+\frac{2R^3}{r^3}\right)\cos\theta + \frac{Q(t)}{4\pi\epsilon r^2}\right]\vec{i}_r - E_0\left[1-\frac{R^3}{r^3}\right]\sin\theta\vec{i}_\theta, \quad r>R, t>0, \tag{1}$$

where $Q(t)$ will be determined in Sec. V. We assume that the net charge on the perfectly conducting sphere is uniformly distributed over the sphere surface.

III. SOLUTION FOR THE ELECTRIC FIELD LINES

With the assumption of small volume charge density so that the resulting electric field from the volume charge is small compared to the applied uniform electric field $\vec{E} = E_0\vec{i}_z$, then $\nabla\cdot\vec{E}\approx 0$. The electric field can then be represented by the curl of a vector potential. With no dependence of the electric field on angle ϕ, the vector potential is of the form $\vec{A}(r,\theta) = A_\phi(r,\theta)\vec{i}_\phi$ and is related to the electric field as[14,15]

$$\vec{E}(r,\theta) = \nabla\times\vec{A}(r,\theta) = \frac{1}{r\sin\theta}\frac{\partial}{\partial\theta}\left(\sin\theta A_\phi\right)\vec{i}_r - \frac{1}{r}\frac{\partial}{\partial r}\left(rA_\phi\right)\vec{i}_\theta. \tag{2}$$

From Eqs. (1) and (2), the vector potential is then

$$A_\phi(r,\theta) = \frac{E_0 r\sin\theta}{2}\left[1+\frac{2R^3}{r^3}\right] - \frac{Q(t)\cos\theta}{4\pi\epsilon r\sin\theta}. \tag{3}$$

Electric field lines are everywhere tangent to the electric field and related to the vector potential of Eq. (3) as

$$\frac{dr}{rd\theta} = \frac{E_r}{E_\theta} = \frac{\frac{1}{r\sin\theta}\frac{\partial}{\partial\theta}\left(\sin\theta A_\phi\right)}{-\frac{1}{r}\frac{\partial}{\partial r}\left(rA_\phi\right)}. \tag{4}$$

After cross multiplication and algebraic reduction of Eq. (4), the electric field lines are lines of constant $\Lambda(r,\theta)$ of the form

$$\Lambda(r,\theta) = r\sin\theta A_\phi(r,\theta) = \frac{E_0 r^2\sin^2\theta}{2}\left[1+\frac{2R^3}{r^3}\right] - \frac{Q(t)\cos\theta}{4\pi\epsilon}, \tag{5}$$

where $\Lambda(r,\theta)$ is called the stream function with

$$d(\Lambda(r,\theta)) = d\left(r\sin\theta A_\phi(r,\theta)\right) = \frac{\partial}{\partial r}\left(r\sin\theta A_\phi\right)dr + \frac{\partial}{\partial\theta}\left(r\sin\theta A_\phi\right)d\theta = 0. \tag{6}$$

The solution to Eq. (6) is

$$\Lambda(r,\theta) = \text{constant} = \Lambda(r_0,\theta_0) = r_0\sin\theta A_\phi(r_0,\theta_0), \tag{7}$$

where (r_0, θ_0) is a specified point that the field line, also called a streamline, passes through. The electric field line passing through the specified point (r_0, θ_0) is then

$$\frac{E_0 r^2\sin\theta}{2}\left[1+\frac{2R^3}{r^3}\right] - \frac{Q(t)\cos\theta}{4\pi\epsilon} = \frac{E_0 r_0^2\sin^2\theta_0}{2}\left[1+\frac{2R^3}{r_0^3}\right] - \frac{Q(t)\cos\theta_0}{4\pi\epsilon}. \tag{8}$$

IV. CRITICAL POINTS

Positive charge can only be deposited on the sphere where the radial component of the electric field is negative, due to negative surface charge on the sphere; while negative

charge can only be deposited on the sphere where the radial component of the electric field is positive, due to positive surface charge on the sphere. The two adjacent charging regions then connect on the sphere at coordinate $(r=R,\ \theta=\theta_c)$, where the radial electric field is zero, i.e., $E_r(r=R,\ \theta=\theta_c)=0$. θ_c is the critical polar angle on the sphere and is defined as

$$\cos\theta_c = -\frac{Q(t)}{Q_s}, \tag{9}$$

where

$$Q_s = 12\pi\epsilon E_0 R^2 \tag{10}$$

and Q_s is taken to be positive. The point at coordinate $(r=R,\ \theta=\theta_c)$ is called a critical point because both $E_r(r=R,\ \theta=\theta_c)$ and $E_\theta(r=R,\ \theta=\theta_c)$ are zero. Thus with $E_0>0$, the sphere charges positively for $0<\theta<\theta_c$, where $E_r(r=R,\ \theta)>0$; and charges negatively for $\theta_c<\theta<\pi$, where $E_r(r=R,\ \theta)<0$.

Letting $(r_0=R,\ \theta_0=\theta_c)$ be the specified point that the field line passes through, the equation of this special separation field line is

$$\begin{aligned}\Lambda(r,\theta) &= \Lambda(r=R,\theta=\theta_c)\\ &= \frac{E_0 r^2\sin^2\theta}{2}\left[1+\frac{2R^3}{r^3}\right]-\frac{Q(t)\cos\theta}{4\pi\epsilon}\\ &= \frac{3E_0R^2\sin^2\theta_c}{2}-\frac{Q(t)\cos\theta_c}{4\pi\epsilon}\\ &= \frac{3E_0R^2}{2}\left[1+\left(\frac{Q(t)}{Q_s}\right)^2\right],\end{aligned} \tag{11}$$

where the last equality is obtained using Eqs. (9) and (10). This special field line separates field lines starting at $z\to\pm\infty$ that terminate on the sphere from field lines that go around the sphere.

Evaluating Eq. (11) at $r\to\infty$ $\theta\to 0$ [i.e., $\Lambda(r=R,\theta=\theta_c)=\Lambda(r\to\infty,\theta\to 0)$] gives the cylindrical radius $R_a(t)$ for negative charges at $z\to\pm\infty$, which terminate on the upper part of the sphere for $0<\theta<\theta_c$.

$$R_a(t) = \lim_{\substack{r\to\infty\\ \theta\to 0}}(r\sin\theta) = \sqrt{3}R\left[1+\frac{Q(t)}{Q_s}\right]. \tag{12}$$

Similarly, evaluating Eq. (11) at $r\to\infty$, $\theta\to\pi$ [i.e., $\Lambda(r=R,\theta=\theta_c)=\Lambda(r\to\infty,\theta\to\pi)$] gives the cylindrical radius $R_b(t)$ for positive charges at $z\to-\infty$, which terminate on the lower part of the sphere for $\theta_c<\theta<\pi$.

$$R_b(t) = \lim_{\substack{r\to\infty\\ \theta\to\pi}}(r\sin\theta) = \sqrt{3}R\left[1-\frac{Q(t)}{Q_s}\right]. \tag{13}$$

At $t=0$, when $Q(t=0)=0$, such that the sphere is initially uncharged, then

$$R_a(t=0) = R_b(t=0) = \sqrt{3}R. \tag{14}$$

V. TOTAL CURRENT THAT CHARGES THE SPHERE

The total current due to positive and negative mobile ions and ohmic conduction that charge the sphere is then

$$\begin{aligned}I &= \frac{dQ(t)}{dt}\\ &= 2\pi R^2\left\{\int_{\theta=0}^{\theta_c}\rho_-\mu_-E_r(r=R)\sin\theta d\theta-\int_{\theta=\theta_c}^{\pi}\rho_+\mu_+E_r(r=R)\sin\theta d\theta-\int_{\theta=0}^{\pi}\sigma E_r(r=R)\sin\theta d\theta\right\}\\ &= \frac{Q_s}{4\epsilon}\left\{\left(\rho_+\mu_++\rho_-\mu_-\right)\left[1+\left(\frac{Q(t)}{Q_s}\right)^2\right]-2\left(\rho_+\mu_--\rho_-\mu_-\right)\frac{Q(t)}{Q_s}-\frac{4\sigma Q(t)}{Q_s}\right\},\end{aligned} \tag{15}$$

where

$$E_r(r=R) = 3E_0\cos\theta+\frac{Q(t)}{4\pi\epsilon R^2} \tag{16}$$

is obtained from Eq. (1). Then Eq. (15) can be rewritten as

$$\frac{d}{dt}\left(\frac{Q(t)}{Q_s}\right) = \frac{1}{\tau}\left\{\Sigma\left[1+\left(\frac{Q(t)}{Q_s}\right)^2\right]-2\left(\frac{Q(t)}{Q_s}\right)\right\}, \tag{17}$$

where

$$\tau = \frac{4\epsilon}{\rho_+\mu_+-\rho_-\mu_-+2\sigma}, \tag{18a}$$

$$\Sigma = \frac{\rho_+\mu_++\rho_-\mu_-}{\rho_+\mu_+-\rho_-\mu_-+2\sigma}. \tag{18b}$$

Note that in Eqs. (18a) and (18b) all quantities on the right are positive except for ρ_- so that $\tau>0$ and $-1\le\Sigma\le 1$. The nondimensional charge $(Q(t)/Q_s)$ can then be found by integrating Eq. (17) subject to the initial condition that $Q(t=0)=0$

$$\frac{Q(t)}{Q_s} = \frac{1}{\Sigma}\left\{1-\sqrt{1-\Sigma^2}\tanh\left[\frac{t}{\tau}\sqrt{1-\Sigma^2}+\operatorname{arctanh}\left(\frac{1}{\sqrt{1-\Sigma^2}}\right)\right]\right\}. \tag{19}$$

Note that in Eq. (19) the initial and steady-state solutions are

$$\frac{Q(t=0)}{Q_s} = 0, \tag{20a}$$

$$\frac{Q(t\to\infty)}{Q_s} = \frac{1-\sqrt{1-\Sigma^2}}{\Sigma}. \tag{20b}$$

The steady-state sphere charge is positive if Σ is positive ($\rho_+\mu_+ > -\rho_-\mu_-$) and is negative if Σ is negative ($-\rho_-\mu_- > \rho_+\mu_+$). Also, for $|\Sigma| < 1$, that is not including the unipolar charging ($\rho_+\mu_+ = 0$ or $\rho_-\mu_- = 0$) with lossless dielectric medium ($\sigma = 0$) cases, where $\Sigma = \pm 1$, the steady-state sphere charge magnitude is always less than Q_s [i.e., $|Q(t \to \infty)| < Q_s$], resulting in a lower saturation charge.

Using Eq. (20) in Eqs. (12) and (13), the steady-state (i.e., $t \to \infty$) cylindrical radii at $z \to \pm\infty$ are

$$R_a(t \to \infty) = \sqrt{3}R\left(\frac{\Sigma + 1 - \sqrt{1-\Sigma^2}}{\Sigma}\right), \tag{21a}$$

$$R_b(t \to \infty) = \sqrt{3}R\left(\frac{\Sigma - 1 + \sqrt{1-\Sigma^2}}{\Sigma}\right), \tag{21b}$$

where Σ is given in Eq. (18b).

VI. ANOTHER METHOD TO CHECK THE SPHERE CHARGING CURRENT

The difference in the current that charges the sphere at $z \to -\infty$ for $0 < r \sin\theta < R_b(t)$ and at $z \to +\infty$ for $0 < r \sin\theta < R_a(t)$ must equal the current of Eq. (15) that charges the sphere. This provides a simple check of Eq. (15) because at $z \to \pm\infty$ the electric field is uniform, $\vec{E} = E_0\vec{i}_z$, so the z-directed current densities for sphere positive charging, $\vec{J}_+(z \to -\infty)$, and sphere negative charging, $\vec{J}_-(z \to +\infty)$, including ohmic current contributions, are also uniform.

$$\vec{J}_+(z \to -\infty) = (\rho_+\mu_+ + \sigma)E_0\vec{i}_z \tag{22a}$$

$$\vec{J}_-(z \to +\infty) = (-\rho_-\mu_- + \sigma)E_0\vec{i}_z. \tag{22b}$$

The total charging current is obtained by multiplying the current density $\vec{J}_+(z \to -\infty)$ by the area $\pi R_b{}^2(t)$ and multiplying the current density $\vec{J}_-(z \to +\infty)$ by $\pi R_a{}^2(t)$. Then taking the difference of the two current contributions using Eqs. (12) and (13) yields

$$\begin{aligned} I &= \frac{dQ(t)}{dt} \\ &= \left[\vec{J}_+(z \to -\infty)\pi R_b^2(t) - \vec{J}_-(z \to +\infty)\pi R_b^2(t)\right] \cdot \vec{i}_z \\ &= 3\pi R^2 E_0 \left\{ (\rho_+\mu_+ + \rho_-\mu_-)\left[1 + \left(\frac{Q(t)}{Q_s}\right)^2\right] \right. \\ &\quad \left. - 2\left(\rho_+\mu_+ - \rho_-\mu_- + 2\sigma\right)\frac{Q(t)}{Q_s}\right\}. \end{aligned} \tag{23}$$

The charging current given in Eq. (23) matches that in Eq. (15), where we recognize that

$$3\pi R^2 E_0 = \frac{Q_s}{4\epsilon}. \tag{24}$$

VII. UNIPOLAR CHARGING OF THE SPHERE

A. Positive charging

The negative charge does not contribute to the charging current of the sphere if either ρ_- or μ_- is zero. Then for positive charging, Eq. (18) reduces to

$$\tau = \frac{2\tau_+\tau_s}{\tau_+ + 2\tau_s} \tag{25a}$$

$$\Sigma = \frac{2\tau_s}{\tau_+ + 2\tau_s}, \tag{25b}$$

where

$$\tau_+ = \frac{4\epsilon}{\rho_+\mu_+}, \tag{26a}$$

$$\tau_s = \frac{\epsilon}{\sigma}, \tag{26b}$$

are the positive mobile charge and ohmic relaxation time constants. If the dielectric medium is perfectly insulating, $\sigma = 0$, then $\tau_s \to \infty$ so that Eqs. (19) and (25) greatly reduce to

$$\tau = \tau_+, \tag{27a}$$

$$\Sigma = 1, \tag{27b}$$

and

$$\frac{Q(t)}{Q_s} = \frac{t}{t + \tau_+}. \tag{28}$$

B. Negative charging

The positive charge does not contribute to the charging current of the sphere if either ρ_+ or μ_+ is zero. Then for negative charging, Eq. (18) reduces to

$$\tau = \frac{2\tau_-\tau_s}{\tau_- + 2\tau_s} \tag{29a}$$

$$\Sigma = \frac{-2\tau_s}{\tau_- + 2\tau_s} \tag{29b}$$

where

$$\tau_- = \frac{-4\epsilon}{\rho_-\mu_-} = \frac{4\epsilon}{|\rho_-|\mu_-} \tag{30a}$$

$$\tau_s = \frac{\epsilon}{\sigma}, \tag{30b}$$

are the negative mobile charge and ohmic relaxation time constants. Note, the magnitude of negative charge density, $|\rho_-|$, is used in Eq. (30a) because ρ_- is a negative number so that τ_- is positive. If the dielectric medium is perfectly insulating, $\sigma = 0$, then $\tau_s \to \infty$ so that Eqs. (19) and (29) greatly reduce to

$$\tau = \tau_-, \tag{31a}$$

$$\Sigma = -1, \tag{31b}$$

and

$$\frac{Q(t)}{Q_s} = \frac{-t}{t + \tau_-}. \tag{32}$$

Figure 2 plots unipolar positive charging described by Eqs. (25)–(28) for various values of τ_s/τ_+ and unipolar negative

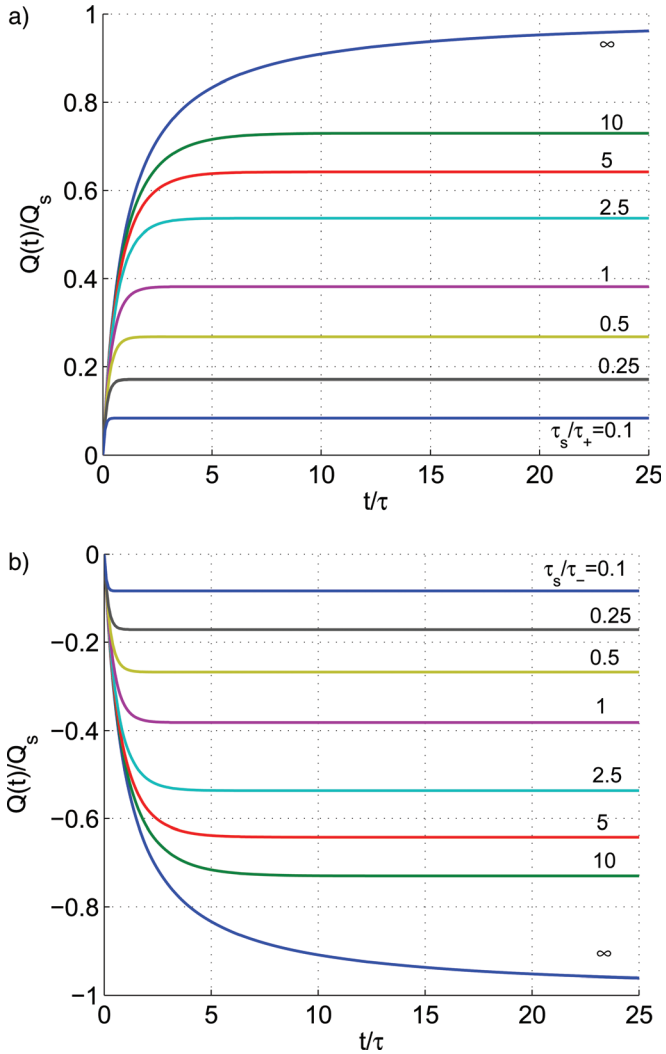

FIG. 2. (Color online) Unipolar charging of a perfectly conducting sphere versus time for (a) positive mobile charge ($\rho_-\mu_- = 0$ for various values of τ_s/τ_+) and for (b) negative mobile charge ($\rho_+\mu_+ = 0$ for various values of τ_s/τ_-). Note that the (a) positive charge plot has $Q(t) > 0$ for all time with time constant τ given by Eq. (25a), while the (b) negative charge plot has $Q(t) < 0$ for all time with time constant τ given by Eq. (29a).

charging described by Eqs. (29)–(32) for various values of τ_s/τ_-. When $\tau_s \to \infty$ the positive charging is given by Eq. (28) and the negative charging is given by Eq. (32).

Figure 3 plots the electric field lines for positive unipolar conduction in a lossless dielectric, $\sigma = 0$, by taking either $\rho_- = 0$ or $\mu_- = 0$ for values of $\theta_c = \pi/2$, $2\pi/3$, $5\pi/6$, and π. The electric field line plots for negative unipolar conduction (i.e., $\rho_+ = 0$ or $\mu_+ = 0$) in a lossless dielectric, $\sigma = 0$, can be found in Ref. 13. The negative unipolar conduction model in a lossless dielectric was used in Ref. 13 to model the electron capturing capability of conductive nanoparticles, such as magnetite, in transformer oil. In particular, these nanoparticles were shown to enhance the electrical breakdown performance of transformer oil by effectively capturing mobile electrons that are created via ionization and converting them to slow moving negatively charged nanoparticles, which inhibits the development of space charge in the oil. The use of the negative unipolar model is a simplification as the transformer oil has a nonzero conductivity and the existence of positive charge carriers formed during ionization. The next section will examine the effect of generalizing this model to include these factors and the impact charging capability of such nanoparticles and the breakdown performance of transformer oil-based nanofluids.

VIII. BIPOLAR CHARGING OF THE SPHERE

We consider in Fig. 4 the charge $Q(t)/Q_s$ and critical charging polar angle $\theta_c(t)$ of the perfectly conducting sphere as a function of time for bipolar charging and various values of Σ. For example, $\Sigma > 0$ models $\rho_+\mu_+ > -\rho_-\mu_-$ for positive charging [Figs. 4(a) and (b)] and approaches the positive unipolar case when $\Sigma = 1$. On the other hand, $\Sigma < 0$ models $-\rho_-\mu_- > \rho_+\mu_+$ for negative charging [Fig. 4(c) and (d)] and approaches the negative unipolar case when $\Sigma = -1$. Note that the positive charge plot in Fig. 4(a) has $\rho_+\mu_+ > -\rho_-\mu_-$ so that $Q(t) > 0$ for all time, while the negative charge plot in Fig. 4(c) has $-\rho_-\mu_- > \rho_+\mu_+$ so that $Q(t) < 0$ for all time. Also, notice that the case when $\Sigma = 0$, that is $-\rho_-\mu_- = \rho_+\mu_+$, there is no net charging of the sphere, $Q(t) = 0$, as the charges on the top and bottom halves of the sphere have equal magnitude but opposite sign.

The charge magnitude on the sphere $|Q(t)|$ for $|\Sigma| < 1$ [Figs. 4(a) and (c)] is always less than Q_s. Even at steady-state (i.e., $t \to \infty$ the sphere charge saturates to less than Q_s (i.e., $|Q(t)| < Q_s$ for $|\Sigma| < 1$). As a result, the critical angle $\theta_c(t)$, which is defined by $\cos\theta_c(t) = -Q(t)/Q_s$ in Eq. (9) and is bounded by $0 < \theta_c(t) < \pi$, at steady-state will not reach 0 or π and the sphere will be at an equilibrium charging, where the surface charging of the sphere by positive and negative charges plus the discharging of the sphere via the lossy dielectric medium will be equal. For example, Fig. 5 examines the electric field lines around a perfectly conducting sphere in a dielectric medium when $\Sigma = 0.95$, such that $\rho_+\mu_+ > -\rho_-\mu_-$ and $Q(t > 0) > 0$. At first glance, comparing Fig. 5(a) with the unipolar positive charging of a sphere in a lossless dielectric medium, as shown in Fig. 3(a), at $t = 0$ the sphere remains uncharged due to the finite conductivity of the dielectric medium and free charges. However, at later times for the $\Sigma = 0.95$ case the sphere charges and has a net positive charge.

For $t > 0$, comparing the bipolar charging ($\Sigma = 0.95$) of the sphere in Fig. 5 with that of the unipolar ($\Sigma = 1$) positive charging case in Fig. 3, two things are evident. First, the net positive charging of the sphere in the bipolar charging case occurs more slowly, as it takes approximately 1.159τ [Fig. 5(c)] for the sphere to charge to $0.5Q_s$, while in the unipolar charging, lossless dielectric case reaching the same charge only takes τ [Fig. 3(b)]. This occurs because both positive and negative charge carriers exist in the dielectric medium and ultimately charge the sphere. As the negative charge carriers, with their lower conductivity than their positive counterparts (i.e., $\rho_+\mu_+ > -\rho_-\mu_-$), charge the sphere they decrease the net positive sphere charge, which results in longer charging times. Furthermore, due to the nonzero conductivity, σ, of the surrounding dielectric medium, there exists a path for the sphere surface charge to discharge back to the dielectric, lowering the total sphere charge.

The second observation is that as $t \to \infty$ the sphere reaches a saturation charge less than Q_s [Fig. 5(d)] and its

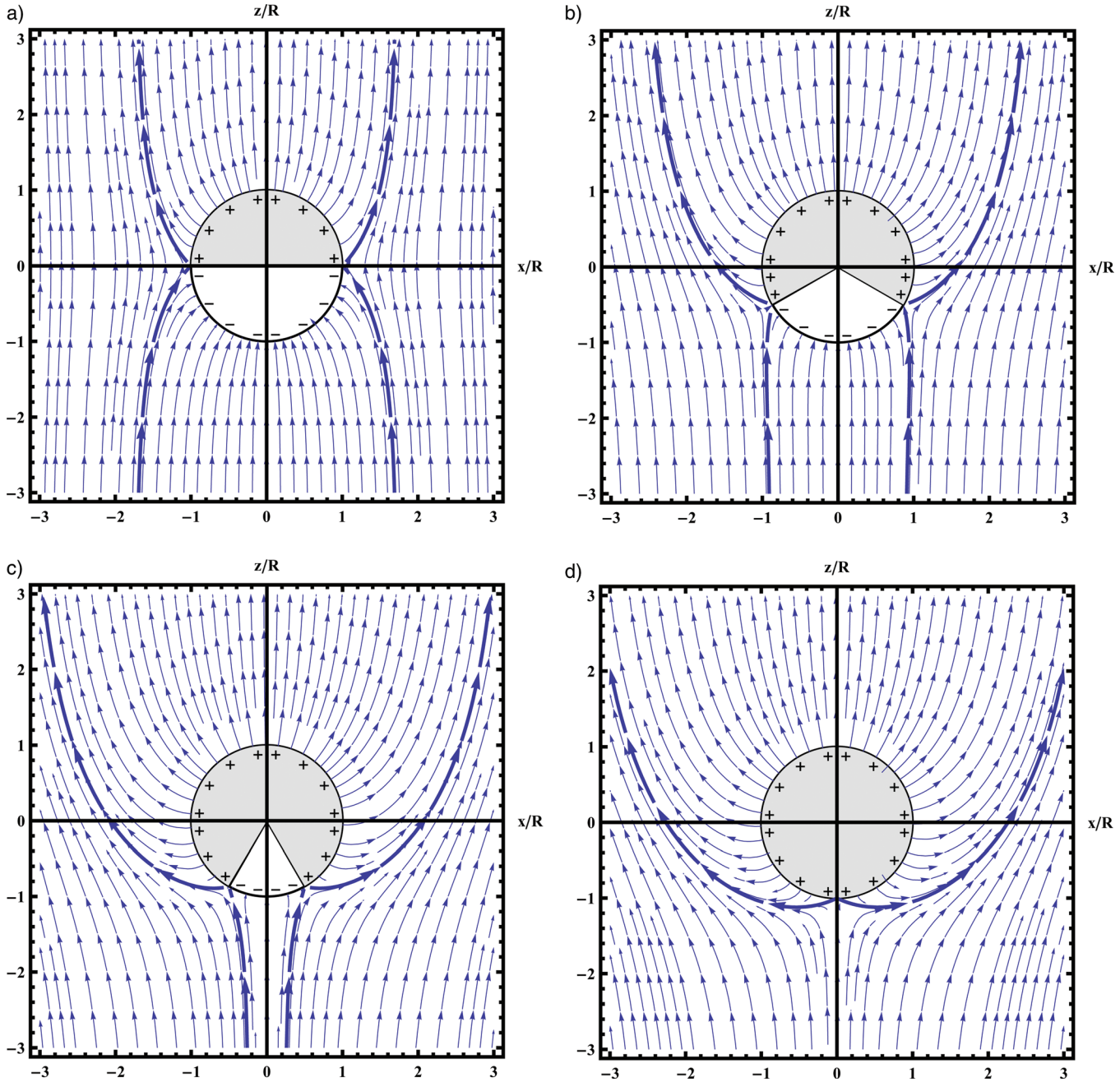

FIG. 3. (Color online) Electric field lines for various times after a uniform z-directed electric field is turned on at $t=0$ around a perfectly conducting sphere of radius R surrounded by a lossless dielectric with permittivity ϵ, conductivity $\sigma=0$, and free mobile positive charge with uniform positive charge density ρ_+ and mobility μ_+, and zero negative charge current such that $\rho_-\mu_-=0$. The thick electric field lines terminate on the particle at $r=R$ and $\theta=\theta_c$, where $E_r(r=R)=0$, and separate field lines that terminate on the sphere from field lines that go around the sphere. The cylindrical radius $R_b(t)$ of Eq. (13) of the separation field line at $z\rightarrow-\infty$ defines the positive mobile charge current $I(t)$ in Eq. (23) with $\rho_-\mu_-=0$ and $\sigma=0$. The cylindrical radius $R_a(t)$ of Eq. (12) defines the separation field line at $z\rightarrow+\infty$. The electric field lines in this figure were plotted using Mathematica StreamPlot (Ref. 16). (a) $\theta_c=\pi/2$, $t/\tau_+=0$, $Q\,(t=0)/Q_s=0$, $R_a\,(t)/R=R_b\,(t)/R=\sqrt{3}$; (b) $\theta_c=2\pi/3$, $t/\tau_+=1$, $Q\,(t=\tau_+)/Q_s=1/2$, $R_a\,(t)/R=3\sqrt{3}/2$, $R_b\,(t)/R=\sqrt{3}/2$; (c) $\theta_c=5\pi/6$, $t/\tau_+\approx 6.464$, $Q\,(t=6.464\tau_+)/Q_s=\sqrt{3}/2$, $R_a\,(t)/R\approx 3.232$, $R_b\,(t)/R\approx 0.232$; and (d) $\theta_c=\pi$, $t/\tau_+\rightarrow\infty$, $Q\,(t\rightarrow\infty)/Q_s=1$, $R_a\,(t)/R=2\sqrt{3}$, $R_b\,(t)/R=0$.

critical angle is $\theta_c\approx 2.380<\pi$, such that a portion of its surface area ($\theta<\theta_c$) is continually being charged by negative free charges, while the other remaining surface area ($\theta>\theta_c$) is charged by positive free charges from the dielectric medium. This is in contrast to the unipolar positive charging case in a lossless dielectric where the sphere charges to Q_s resulting in no electric field lines terminating on the surface and, consequently, no further charging on the sphere by free positive charge [Fig. 3(d)]. In the bipolar charging case, the lower saturation charge occurs because as the sphere charges, which leads to a greater net positive charge, the sphere's surface area, where electric field lines terminate, decreases and hence, the area for positive charging decreases. Conversely, the surface area on the sphere where electric field lines emanate from is increased and, consequently, the surface area for negative charge carriers to charge the sphere has increased. So even though the free positive charge carriers may have a greater conductivity (i.e.,

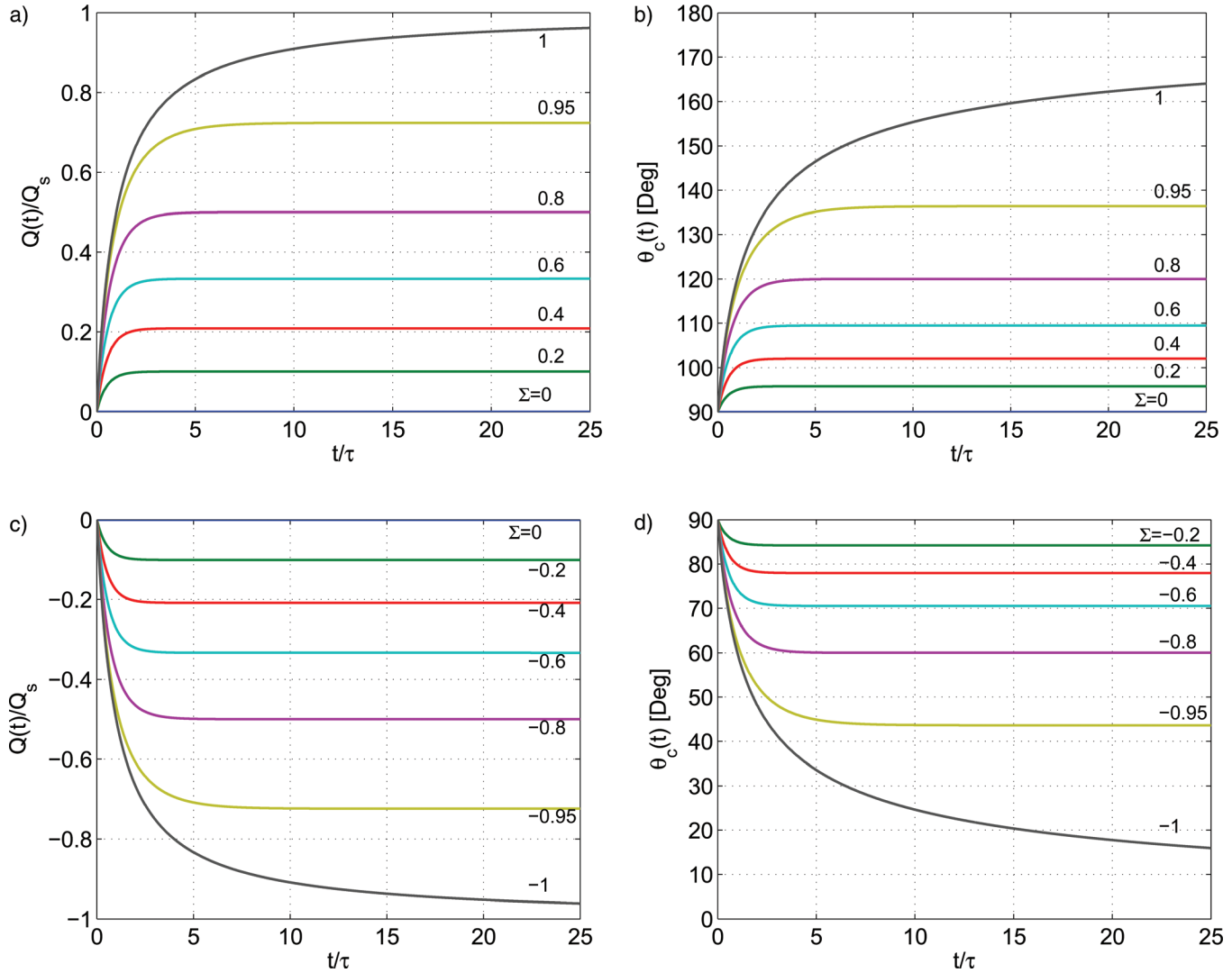

FIG. 4. (Color online) The charge $Q(t)/Q_s$ and critical charging polar angle $\theta_c(t)$ of a perfectly conducting sphere for bipolar charging versus time for various values of Σ from Eq. (18b). (a), (b) $0 \leq \Sigma \leq 1$ (i.e., $\rho_+\mu_+ > -\rho_-\mu_-$) for positive charging and (c), (d) $-1 \leq \Sigma \leq 0$ (i.e., $-\rho_-\mu_- > \rho_+\mu_+$) for negative charging.

greater charge density and/or mobility) than the negative charge carriers, there comes a point that the greater positive charge conductivity is offset by lower surface charging area and the total rate of positive to negative carrier charging plus the discharge rate of sphere charge via the lossy dielectric medium comes to an equilibrium, where the charging current I in Eq. (15) equals zero and the charge on the sphere reaches its lowered charge saturation level.

The effect of varying positive and negative charge carrier conductivities and the nonzero conductivity of the dielectric medium on the sphere saturation charge and critical angle is captured in Fig. 6. For $0.5 < |\Sigma| \leq 1$, there is a great change in the sphere saturation charge from $0.268Q_s$ to Q_s, while for $|\Sigma| \leq 0.5$ the change in saturation charge is much more gradual and almost linear. In Fig. 7, steady-state electric field line plots are shown for $\Sigma = -2\sqrt{2}/3$ and $2\sqrt{2}/3$. The saturation charge for each case is $Q(t \to \infty) = -1/\sqrt{2}$ and $1/\sqrt{2}$, respectively. The figure also captures the differences in electric field line orientation for negative and positive charging of the sphere.

This section has shown how the existence of both positive and negative charges, and especially their relative conductivities, affects the charging of a perfectly conducting sphere in a lossy dielectric medium. But these conductivities do not only affect the sphere's charging dynamics, saturation charge, and critical angle, they also affect the cylindrical radii R_a and R_b at $z \to \pm\infty$ that define the electric field lines that emanate and terminate on the sphere. Figure 8 plots these cylindrical radii as a function of time for several different Σ. As $|\Sigma|$ increases, the change from the no charge initial condition of $R_a(t=0) = R_b(t=0) = \sqrt{3}R$ increases as well.

The analysis of this section has an impact on the unipolar negative charge capturing model presented in Ref. 13 for conductive nanoparticles in transformer oil, which was used to explain the improved electrical breakdown performance due to electron scavenging in the ionization region. By generalizing the model to include both positive and negative charge carriers and the nonzero conductivity of transformer oil, the nanoparticle saturation charge is lowered and its charging rate is decreased. Therefore, fewer electrons are captured per nanoparticle and it takes longer for charging to occur, thereby limiting the effectiveness of the conductive

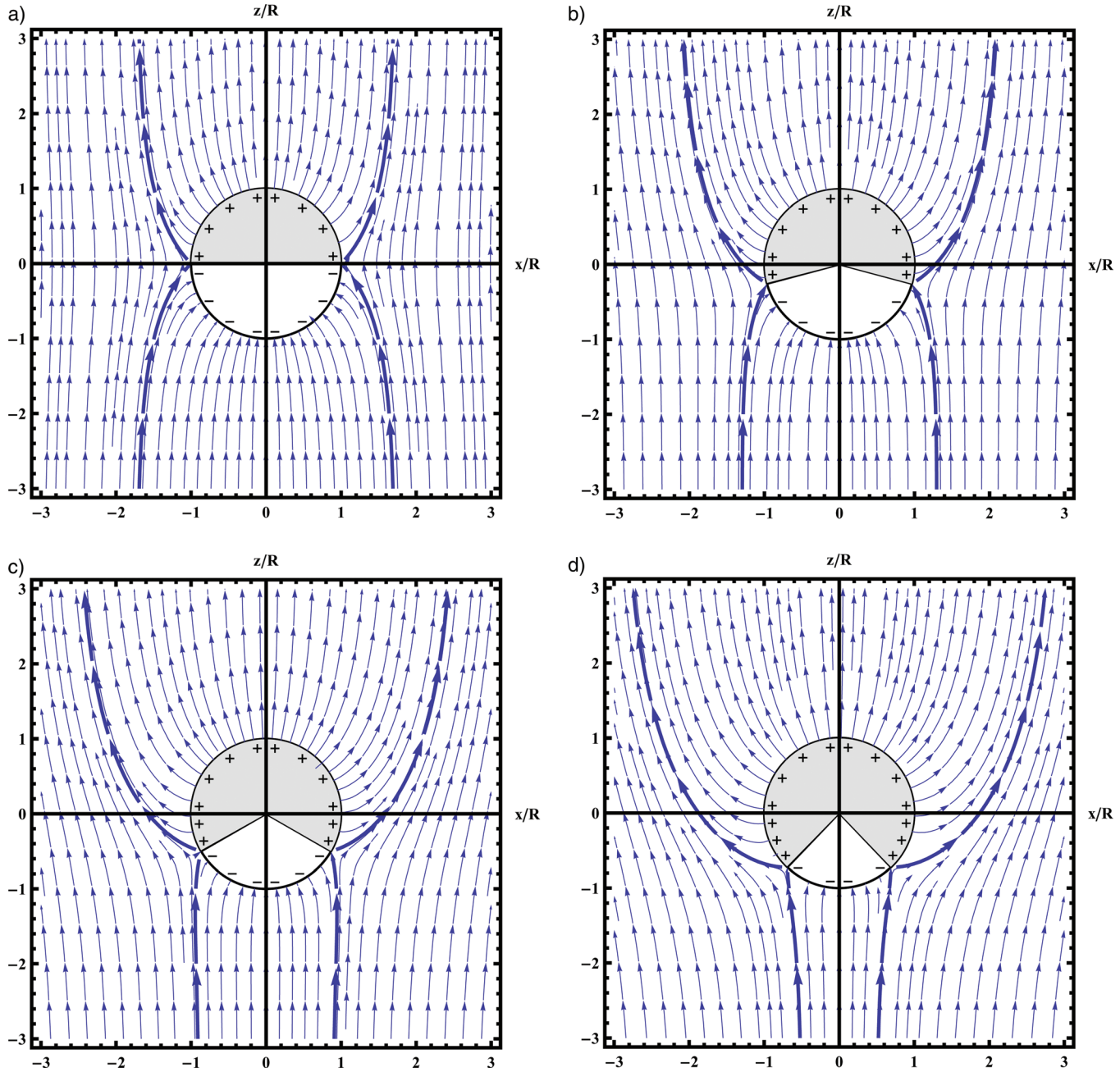

FIG. 5. (Color online) Electric field lines for $\Sigma = 0.95$ and various times after a uniform z-directed electric field is turned on at $t = 0$ around a perfectly conducting sphere of radius R surrounded by a dielectric with permittivity ϵ, conductivity σ, and free mobile positive charge with uniform positive charge density ρ_+ and mobility μ_+, and free mobile negative charge with uniform negative charge density ρ_- and mobility μ_-. The thick electric field lines terminate on the particle at $r = R$ and $\theta = \theta_c$ where $E_r(r = R) = 0$ and separate field lines that terminate on the sphere from field lines that go around the sphere. The cylindrical radius $R_a(t)$ of Eq. (12) describes the separation field line at $z \to +\infty$ and defines the region where negative mobile charge current charges the sphere. The cylindrical radius $R_b(t)$ of Eq. (13) describes the separation field line at $z \to -\infty$ and defines the region where positive mobile charge current charges the sphere. (a) $\theta_c = \pi/2, t/\tau = 0, Q(t = 0)/Q_s = 0, R_a(t)/R = R_b(t)/R = \sqrt{3}$; (b) $\theta_c = 7\pi/12, t/\tau \approx 0.376, Q(t/\tau = 0.376)/Q_s = (\sqrt{3} - 1)/(2\sqrt{2}), R_a(t)/R \approx 2.180, R_b(t)/R \approx 1.284$; (c) $\theta_c = 2\pi/3, t/\tau \approx 1.159, Q(t/\tau = 1.159)/Q_s = 1/2, R_a(t)/R = 3\sqrt{3}/2, R_b(t)/R = \sqrt{3}/2$; and (d) $\theta_c \approx 2.380, t/\tau \to \infty, Q(t \to \infty)/Q_s \approx 0.724, R_a(t)/R \approx 2.986, R_b(t)/R \approx 0.478$.

nanoparticles to improve electrical breakdown performance in transformer oil.

IX. TURN-OFF DISCHARGING TRANSIENTS

A. Ohmic Decay

If the applied field $\vec{E} = E_0 \vec{i}_z$ is suddenly shut off at $t = t_0$ so that $\vec{E}(r \to \infty) = 0$ and the initial sphere charge is $Q(t = t_0)$, we first assume that with no applied field that ionization is prevented, such that $\rho_+ = 0$ and $\rho_- = 0$, and the only current that can flow is ohmic current due to the field of the charged sphere. Then Eqs. (15) and (23) reduce to

$$\frac{dQ(t)}{dt} = -\frac{Q(t)}{\tau_s}, \tag{33}$$

where

$$\tau_s = \frac{\epsilon}{\sigma}. \tag{34}$$

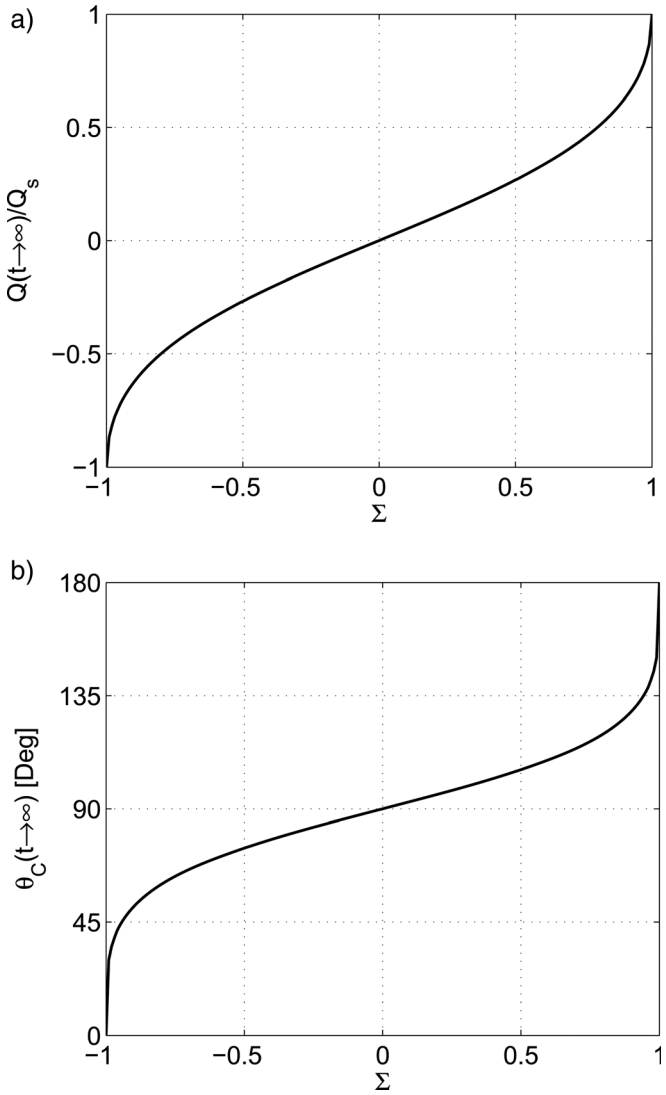

FIG. 6. The perfectly conducting sphere's (a) saturation charge, $Q_a(t \to \infty)/Q_s$ and (b) saturation critical angle as a function of Σ, $\theta_c(t \to \infty)$. Note for non-unipolar cases (i.e., $\Sigma \neq \pm 1$) the sphere does not fully charge to the saturation charge Q_s. Consequently, the critical angle of the charging area will be $0 < \theta_c < \pi$.

The solution to Eq. (33) for $t \geq t_0$ is

$$Q(t \geq t_0) = Q(t = t_0) \exp\left(\frac{-(t - t_0)}{\tau_s}\right) \tag{35}$$

so that the sphere charge decays to zero with time constant τ_s. The electric field is then

$$\begin{aligned} \vec{E}(r > R, t \geq t_0) &= \frac{Q(t \geq t_0)}{4\pi\epsilon r^2}\vec{i}_r \\ &= \frac{Q(t = t_0)}{4\pi\epsilon r^2}\exp\left(\frac{-(t - t_0)}{\tau_s}\right)\vec{i}_r. \end{aligned} \tag{36}$$

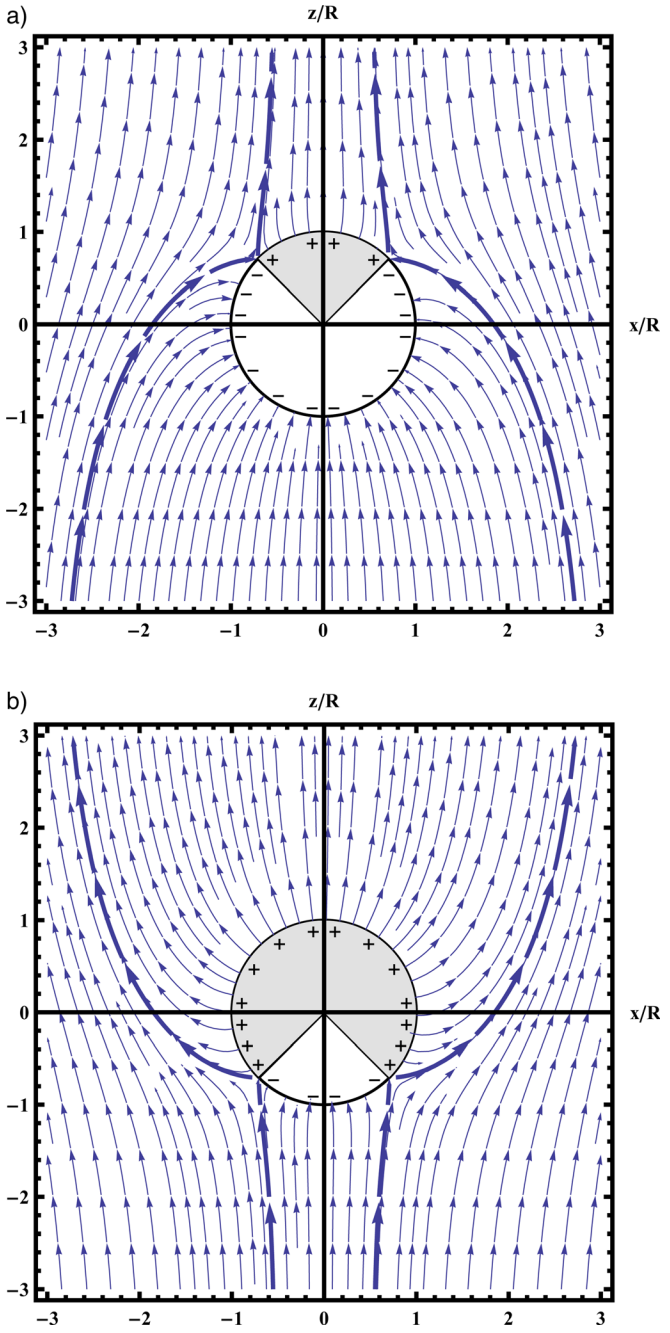

FIG. 7. (Color online) Electric field lines for $t \to \infty$ and opposite polarity values of Σ when a uniform z-directed electric field is applied around a perfectly conducting sphere of radius R surrounded by a dielectric with permittivity ϵ, conductivity σ, and free mobile positive charge with uniform positive charge density ρ_+ and mobility μ_+, and free mobile negative charge with uniform negative charge density ρ_- and mobility μ_-. The thick electric field lines terminate on the particle at $r = R$ and $\theta = \theta_c$ where $E_r(r = R) = 0$ and separate field lines that terminate on the sphere from field lines that go around the sphere. (a) $\Sigma = -2\sqrt{2}/3$, $\theta_c = \pi/4$, $Q(t \to \infty)/Q_s = -1/\sqrt{2}$, $R_a(t)/R = \sqrt{3/2}(\sqrt{2} - 1)$, $R_b(t)/R = \sqrt{3/2}(\sqrt{2} + 1)$; and (b) $\Sigma = 2\sqrt{2}/3$, $\theta_c = 3\pi/4$, $Q(t \to \infty)/Q_s = 1/\sqrt{2}$, $R_a(t)/R = \sqrt{3/2}(\sqrt{2} + 1)$, $R_b(t)/R = \sqrt{3/2}(\sqrt{2} - 1)$.

B. Decay including mobile bipolar charge carriers

Once again, we assume the applied field $\vec{E} = E_0\vec{i}_z$ is suddenly shut off at $t = t_0$ so that $\vec{E}(r \to \infty) = 0$ and the initial sphere charge is $Q(t = t_0)$. However, this time we assume that nonzero mobile bipolar charge carriers continue to exist, such that $\rho_+ \neq 0$ and $\rho_- \neq 0$ in the region outside the sphere with ohmic conductivity σ. In addition to the ohmic current, the mobile charge carriers contribute to the sphere discharging current. There are two cases to consider, dependent on the initial polarity of the sphere's charge $Q(t = t_0)$. The two cases are:

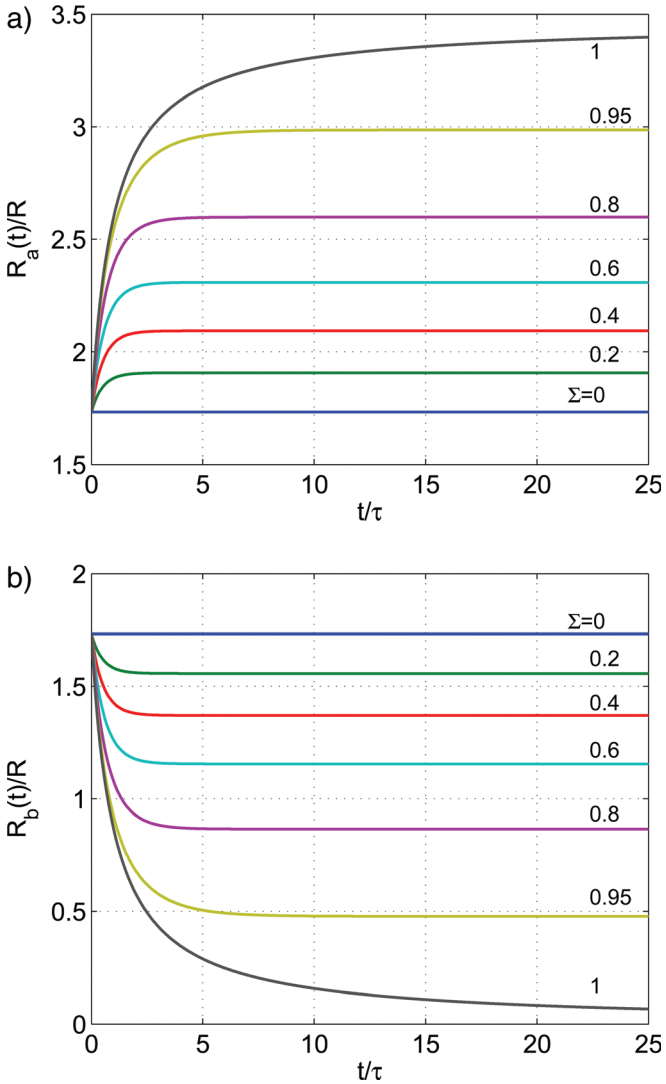

FIG. 8. (Color online) The (a) upper R_a and (b) lower R_b cylindrical radii of the charging window at $z \to \pm\infty$ that charges a perfectly conducting sphere for bipolar charging versus time for various values of $0 \le \Sigma \le 1$ (i.e., $\rho_+\mu_+ > -\rho_-\mu_-$). Note that for $-1 \le \Sigma \le 0$ (i.e., $-\rho_-\mu_- > \rho_+\mu_+$) the upper R_a and lower R_b cylindrical radii are identical to (a) and (b) except that they are interchanged, such that R_a decreases while R_b increases with time and larger $|\Sigma|$.

1. $Q(t = t_0) > 0$

Due to the sphere initial charge being positive, the radial-directed electric field for $r \ge R$ is $\vec{E}_r(r \ge R, t \ge t_0) > 0$, such that the mobile negative charges in the surrounding dielectric are attracted toward the sphere and assist in the discharging of the sphere. The mobile positive charges are repelled and do not contribute in discharging the sphere. The total current due to negative mobile charges and ohmic conduction that discharges the sphere is

$$\begin{aligned} I &= \frac{dQ(t \ge t_0)}{dt} \\ &= 2\pi R^2 \left\{ \int_{\theta=0}^{\pi} \rho_-\mu_- E_r(r=R)\sin\theta d\theta \right. \\ &\quad \left. - \int_{\theta=0}^{\pi} \sigma E_r(r=R)\sin\theta d\theta \right\} \\ &= -\left(\frac{\tau_- + 4\tau_s}{\tau_-\tau_s}\right) Q(t \ge t_0), \end{aligned} \tag{37}$$

where

$$\tau_- = \frac{-4\epsilon}{\rho_-\mu_-} = \frac{4\epsilon}{|\rho_-|\mu_-}, \tag{38a}$$

$$\tau_s = \frac{\epsilon}{\sigma}, \tag{38b}$$

and

$$E_r(r=R) = \frac{Q(t \ge t_0)}{4\pi\epsilon R^2}. \tag{39}$$

The solution to Eq. (37) for $t \ge t_0$ is

$$Q(t \ge t_0) = Q(t = t_0)\exp\left(\frac{-(\tau_- + 4\tau_s)(t - t_0)}{\tau_-\tau_s}\right) \tag{40}$$

so that the positive sphere charge decays to zero with time constant $\tau_-\tau_s/(\tau_- + 4\tau_s)$. The electric field is then

$$\begin{aligned} \vec{E}(r > R, t \ge t_0) &= \frac{Q(t \ge t_0)}{4\pi\epsilon r^2}\vec{i}_r \\ &= \frac{Q(t = t_0)}{4\pi\epsilon r^2}\exp\left(\frac{-(\tau_- + 4\tau_s)(t - t_0)}{\tau_-\tau_s}\right)\vec{i}_r. \end{aligned} \tag{41}$$

If the region surrounding the sphere is perfectly insulating, $\sigma = 0$, so that $\tau_s \to \infty$, the discharge time constant is $\tau_-/4$.

2. $Q(t = t_0) < 0$

This case is analogous to case 1; however, it is shown for completeness. As a result of the initial charge being negative, the radial-directed electric field for $r \ge R$ is $\vec{E}_r(r \ge R, t \ge t_0) < 0$ such that the mobile positive charges in the surrounding dielectric are attracted toward the sphere and assist in the discharging of the sphere. The mobile negative charges are repelled and do not assist in discharging the sphere. The total current due to positive mobile charges and ohmic conduction that discharges the sphere is

$$\begin{aligned} I &= \frac{dQ(t \ge t_0)}{dt} \\ &= 2\pi R^2 \left\{ -\int_{\theta=0}^{\pi} \rho_+\mu_+ E_r(r=R)\sin\theta d\theta \right. \\ &\quad \left. - \int_{\theta=0}^{\pi} \sigma E_r(r=R)\sin\theta d\theta \right\} \\ &= -\left(\frac{\tau_+ + 4\tau_s}{\tau_+\tau_s}\right) Q(t \ge t_0), \end{aligned} \tag{42}$$

where

$$\tau_+ = \frac{4\epsilon}{\rho_+\mu_+}, \tag{43a}$$

$$\tau_s = \frac{\epsilon}{\sigma}, \tag{43b}$$

and $E_r(r=R)$ is defined in Eq. (39). The solution to Eq. (42) for $t \ge t_0$ is

$$Q(t \ge t_0) = Q(t = t_0)\exp\left(\frac{-(\tau_+ + 4\tau_s)(t - t_0)}{\tau_+\tau_s}\right), \tag{44}$$

so that the negative sphere charge decays to zero with time constant $\tau_+\tau_s/(\tau_+ + 4\tau_s)$. The electric field is then

$$\vec{E}(r > R, t \geq t_0) = \frac{Q(t \geq t_0)}{4\pi\epsilon r^2}\vec{i}_r = \frac{Q(t = t_0)}{4\pi\epsilon r^2}\exp\left(\frac{-(\tau_+ + 4\tau_s)(t - t_0)}{\tau_+\tau_s}\right)\vec{i}_r. \quad (45)$$

If the region surrounding the sphere is perfectly insulating, $\sigma = 0$, so that $\tau_s \to \infty$, the discharge time constant is $\tau_+/4$.

X. CONCLUSION

This paper extends the analysis on charging and discharging of perfectly conducting spheres in a lossy dielectric medium by a single charge carrier or two charge carriers of opposite polarity. Special cases investigated include unipolar positive and negative charging and discharging and bipolar charging and discharging in a dielectric region with zero and nonzero conductivity. This analysis can be applied to electrical breakdown and streamer propagation in dielectrics with conductive nanoparticle suspensions, thunderstorm electrification, and impact charging in electrostatic precipitators.

From the analysis, a theoretical charging limit is determined, which can be either positive or negative. This saturation charge limit, Q_s, is specified for an applied electric field magnitude, permittivity of the surrounding medium, and sphere size. However, in practice the sphere cannot charge to this limit. Rather the sphere is charged to a lower saturation value due to the nonzero conductivity of the surrounding medium and the existence of both positive and negative charge carriers. Moreover, it is the respective conductivities of these positive and negative carriers, as well as the conductivity of the surrounding medium, which strongly influence the sphere's lowered saturation charge limit, charge polarity, charging rate, and discharging rate. This has a direct impact in specific applications, such as transformer oil-based nanofluids, where conductive spherical nanoparticle suspensions are used for their electron scavenging properties to inhibit positive streamer propagation and electrical breakdown. Due to the nonzero conductivity of transformer oil and the presence of positive ions along with the electrons, the electron scavenging capability of the nanoparticles is reduced and therefore, their effectiveness in decreasing the likelihood of streamers may be limited.

[1]A. Beroual, M. Zahn, A. Badent, K. Kist, A. J. Schwabe, H. Yamashita, K. Yamazawa, M. Danikas, W. G. Chadband, and Y. Torshin, IEEE Electr. Insul. Mag. **14**, 6 (1998).
[2]V. Segal and K. Raj, Indian J. Eng. Mater. Sci. **5**, 416 (1998).
[3]V. Segal, A. Hjorstberg, A. Rabinovich, D. Nattrass, and K. Raj in *IEEE International Symposium on Electrical Insulation ISEI98*, Arlington, VA, 1998, pp. 619–622.
[4]V. Segal, A. Rabinovich, D. Nattrass, K. Raj, and A. Nunes, J. Magn. Magn. Mater. **215**, 513 (2000).
[5]V. Segal, D. Nattrass, K. Raj, and D. Leonard, J. Magn. Magn. Mater. **201**, 70 (1999).
[6]V. Segal, U.S. Patent 5,863,455 (26 January 1999).
[7]K. Raj and R. Moskowitz, U.S. Patent 5,462,685 (31 October 1995).
[8]T. Cader, S. Bernstein, and S. Crowe, U.S. Patent 5,898,353 (27 April 1999).
[9]F. M. O'Sullivan, Ph.D. thesis, Massachusetts Institute of Technology (2007).
[10]J. G. Hwang, Ph.D. thesis, Massachusetts Institute of Technology (2010).
[11]J. G. Hwang, F. O'Sullivan, M. Zahn, O. Hjortstam, L. A. A. Pettersson, and R. Liu in *Conference on Electrical Insulation and Dielectric Phenomena*, Quebec City, Quebec, Canada, 2008, pp. 361–366.
[12]J. G. Hwang, M. Zahn, F. O'Sullivan, L. A. A. Pettersson, O. Hjortstam, and R. Liu in *2009 Electrostatics Joint Conference*, Boston, MA.
[13]J. G. Hwang, M. Zahn, F. O'Sullivan, L. A. A. Pettersson, O. Hjortstam, and R. Liu, J. Appl. Phys. **107**, 014310 (2010).
[14]F. J. W. Whipple and J. A. Chalmers, Q. J. R. Meteorol. Soc. **70**, 103 (1944).
[15]J. R. Melcher, *Continuum Electromechanics* (The MIT Press, Cambridge, MA, 1981).
[16]For more information about Mathematica StreamPlot, see http://reference.wolfram.com/mathematica/ref/StreamPlot.html.